

# Semiclassical treatment of fusion and breakup processes of ${}^6,8\text{He}$ halo nuclei

Fouad A. Majeed<sup>1</sup>  · Yousif A. Abdul-Hussien<sup>1</sup>

Received: 6 July 2015 / Accepted: 20 December 2015  
© The Author(s) 2016. This article is published with open access at Springerlink.com

**Abstract** A semiclassical approach has been used to study the effect of channel coupling on the calculations of the total fusion reaction cross section  $\sigma_{\text{fus}}$ , and the fusion barrier distribution  $D_{\text{fus}}$  for the systems  ${}^6\text{He} + {}^{238}\text{U}$  and  ${}^8\text{He} + {}^{197}\text{Au}$ . Since these systems involves light exotic nuclei, breakup states channel play an important role that should be considered in the calculations. In semiclassical treatment, the relative motion between the projectile and target nuclei is approximated by a classical trajectory while the intrinsic dynamics is handled by time-dependent quantum mechanics. The calculations of the total fusion cross section  $\sigma_{\text{fus}}$ , and the fusion barrier distribution  $D_{\text{fus}}$  are compared with the full quantum mechanical calculations using the coupled-channels calculations with all order coupling using the computer code and with the available experimental data.

**Keywords** Coupled channels · Fusion reactions · Fusion barrier distribution

## Introduction

The effects of channel coupling in fusion reactions induced by light weakly bound projectiles have attracted great interest over the last decade [1–3]. Some theoretical

studies predict strong influence of the breakup channel over the complete fusion (CF) cross section [4–10]. This has primarily been motivated by the present availability of radioactive ion beams, some of which exhibit unusual features like halo/skin structure and large breakup probabilities. A critical understanding of the fusion mechanism with radioactive ion beams is very significant for the understanding of reactions of astrophysical interest and for the production of new nuclei near the drip lines [11–19]. The natural theoretical tool for their description is the coupled-channel method. However, when a weakly bound collision partner is involved, breakup states channel play an important role. Since they are in the continuum, an infinite number of channels should be taken into account. To handle this situation, the continuum can be discretized by the continuum discretized coupled-channel method (CDCC). However, the method is very complicated and requires considerable computer power. For practical purposes, it becomes necessary to approximate the continuum by a finite set of states, as in the CDCC method [20–23]. This procedure has been extended to the case of fusion reactions in Refs. [8–10]. A semiclassical treatment alternative based on the classical trajectory approximation of Alder and Winther (AW) [24] has been proposed by Marta et al. [25].

The aim of the present work focuses on using a semiclassical approach by adopting Alder and Winther (AW) theory originally used to treat the Coulomb excitation of nuclei. The approximation of AW consists of using classical mechanics to describe the projectile–target relative motion while the excitation of the extrinsic degrees of the nuclei are described by quantum mechanics. This semiclassical approximation has been implemented and coded in FORTRAN codename (SCF) [26] which has been used to calculate the total fusion cross section  $\sigma_{\text{fus}}$  (mb) and the

✉ Fouad A. Majeed  
fouadalajeeli@yahoo.com; fouadattia@gmail.com  
Yousif A. Abdul-Hussien  
yousifhakeemaltamem@yahoo.com

<sup>1</sup> Present Address: Department of Physics, College of Education for Pure Sciences, University of Babylon, Hillah, Iraq

fusion barrier distribution  $D_{\text{fus}}$  (mb/MeV) for the systems involving light exotic nuclei  ${}^6\text{He} + {}^{238}\text{U}$  and  ${}^8\text{He} + {}^{197}\text{Au}$ . The results of the present study are compared to the full quantum mechanical calculations using the coupled-channel calculations (CC) using the computer code CCFULL [27] and with the available experimental data.

### Theoretical framework

Since this work is mainly concerned with the reactions induced by weakly bound projectiles, two variables have been employed, namely  $\mathbf{r}$  and  $\xi$  for the projectile–target separation vector and the relevant intrinsic degrees of freedom of the projectile, respectively. The internal structure for the target nucleus have been neglected for simplicity. The Hamiltonian then reads

$$H = H_0(\xi) + V(\mathbf{r}, \xi) \tag{1}$$

where  $H_0(\xi)$  is the intrinsic Hamiltonian of the projectile and  $V(\mathbf{r}, \xi)$  represents the projectile–target interaction. The eigenvectors of  $H_0(\xi)$  are given by the equation

$$H_0|\psi_v\rangle = \epsilon_v|\psi_v\rangle \tag{2}$$

The AW theory [24] is implemented in the following sequence: first, classical mechanics has been used for the time evolution of the variable,  $r$ . The trajectory depends on the collision energy,  $E$ , the angular momentum,  $\hbar\ell$ . The Rutherford trajectory  $r_\ell(t)$  was used in the original AW method. In our case, the solution of the trajectory is the equations of classical motion with the potential,  $V(r) = \langle\psi_0|V(r, \xi)|\psi_0\rangle$  where  $|\psi_0\rangle$  is a wave function of the ground state of the projectile. The coupling interaction becomes a time-dependent interaction at using the  $\xi$ -space,  $V(r_\ell(t), \xi)$ . Second, the dynamics were treated in the intrinsic space as a time-dependent quantum mechanics problem. Expanding the wave function in the basis of intrinsic eigen states,

$$\Psi(\xi, t) = \sum_v A_v(\ell, t)\psi_v(\xi)e^{-i\epsilon_v t/\hbar} \tag{3}$$

and inserting this expansion into the time-dependent Schrödinger equation for  $\Psi(\xi, t)$ , one obtains the AW coupled equations

$$i\hbar \frac{\partial A_v(\ell, t)}{\partial t} = \sum_\mu \langle\psi_v|V_\ell(\xi, t)|\psi_\mu\rangle e^{-i(\epsilon_v - \epsilon_\mu)t/\hbar} A_\mu(\ell, t) \tag{4}$$

These equations are solved with the initial conditions  $A_v(\ell, t \rightarrow -\infty) = \delta_{v,0}$ , which means that before the collision ( $t \rightarrow -\infty$ ) the projectile was in its ground state. The final population of channel  $v$  in a collision with angular

momentum  $\ell$  is  $P_\ell^{(v)} = |A_v(\ell, t \rightarrow +\infty)|^2$  and the angle integrated cross section is:

$$\sigma_v = \frac{\pi}{k^2} \sum_\ell (2\ell + 1) P_\ell^{(v)} \tag{5}$$

For using this method in the fusion processes, we start with the quantum mechanical calculation of the fusion reaction cross section in a coupled-channel problem. It is assumed that all the channels are bound and have spin zero for simplicity. The fusion reaction cross section is a sum of contributions from each channel. Carrying out partial-wave expansions we get

$$\sigma_F = \sum_v \left[ \frac{\pi}{k^2} \sum_\ell (2\ell + 1) P_\ell^F(v) \right] \tag{6}$$

with

$$P_\ell^F(v) = \frac{4k}{E} \int |U_{v\ell}(k_v, r)|^2 W_v^F(r) dr \tag{7}$$

Above,  $U_{v\ell}(k_v, r)$  represents the radial wave function for the  $\ell$ th-partial-wave in channel  $v$  and  $W_v^F(r)$  is the absolute value of the imaginary part of the optical potential associated to fusion reaction in that channel.

To evaluate the fusion cross section using AW method, we had adopted used the approximation:

$$P_\ell^F(v) \simeq \overline{P}_\ell^{(v)} T_\ell^{(v)}(E_v) \tag{8}$$

$\overline{P}_\ell^{(v)}$  is the probability that the system is in channel  $v$  at the point of closest approach on the classical trajectory, and  $T_\ell^{(v)}(E_v)$  is the probability that a particle with energy  $E_v = E - \epsilon_v$  and reduced mass  $\overline{M} = M_p M_T / M_p + M_T$  where  $M_p, M_T$  are, respectively, the masses of the projectile and target, tunnels through the potential barrier in channel  $v$ .

We now proceed to study the CF cross sections in reactions induced by weakly bound projectiles. For simplicity, we assume that the ground state (g.s.) is the only bound state of the projectile and that the breakup process produces only two fragments,  $F_1$  and  $F_2$ . In this way, the labels  $v = 0$  and  $v \neq 0$  correspond, respectively, to the g.s. and the breakup states represented by two unbound fragments. Neglecting any sequential contribution, the CF can only arise from the elastic channel. In this way, the cross section  $\sigma_{CF}$  can be obtained from Eq. (9), dropping contributions from  $v \neq 0$ . That is,

$$\sigma_{CF} = \frac{\pi}{k^2} \sum_\ell (2\ell + 1) P_\ell^{(\text{Surv})} T_\ell^{(0)}(E) \tag{9}$$

where

$$P_\ell^F(v) \equiv \overline{P}_\ell^{(0)} = |A_0(\ell, t_{ca})|^2 \tag{10}$$

### Fusion barrier distribution

The fusion barrier distribution  $D_{\text{fus}}$  is extracted from the measured data of  $\sigma_{\text{fus}}$ , by taking the second derivative, with respect to center of mass energy ( $E_{\text{c.m.}}$ ), of the product ( $E_{\text{c.m.}}\sigma_{\text{fus}}$ ) [28–30] as

$$D_{\text{fus}} = d^2(E_{\text{c.m.}}\sigma_{\text{fus}})/dE_{\text{c.m.}}^2 \tag{11}$$

This quantity is calculated numerically using the three-point difference formula,

$$(D_{\text{fus}})_{i+1} = \frac{2}{E_{i+2} - E_i} \left[ \frac{F_{i+2} - F_{i+1}}{E_{i+2} - E_{i+1}} - \frac{F_{i+1} - F_i}{E_{i+1} - E_i} \right] \tag{12}$$

where

$$F_i = E_i(\sigma_{\text{fus}})_i, i = 1, 2, 3, \dots \tag{13}$$

with equal increments of the energy center of mass  $\Delta E = E_{i+2} - E_{i+1} = E_{i+1} - E_i$ , the numerical formula of  $D_{\text{fus}}$  can be written,

$$(D_{\text{fus}})_{i+1} = \frac{F_{i+2} + F_i - 2F_{i+1}}{\Delta E^2} \tag{14}$$

and the statistical error ( $\delta D_{\text{fus}}$ ) related with the second derivative at energy  $E$  is approximately given by,

$$(\delta D_{\text{fus}})_{i+1} \cong \frac{E_{i+1}}{\Delta E^2} \sqrt{(\delta\sigma_{\text{fus}})_{i+2}^2 + 4(\delta\sigma_{\text{fus}})_{i+1}^2 + (\delta\sigma_{\text{fus}})_i^2} \tag{15}$$

where the  $(\delta\sigma_{\text{fus}})$  are the errors in the fusion interaction cross sections, and  $(\delta D_{\text{fus}})$  is error of the fusion barrier distribution.

### Results and discussion

In this section, the numerical results for the total fusion cross section  $\sigma_{\text{fus}}$ , and the fusion barrier distribution  $D_{\text{fus}}$  calculated using the semiclassical approach for the systems  ${}^6\text{He} + {}^{238}\text{U}$  and  ${}^8\text{He} + {}^{197}\text{Au}$  are explained. Our calculated results of  $\sigma_{\text{fus}}$  and  $D_{\text{fus}}$  are compared with the corresponding experimental data and with the full quantum mechanical calculations using the CCFULL code. The Aküz-Winther potential parameters used in the present calculations are listed in Table 1.

In the case of  ${}^6\text{He} + {}^{238}\text{U}$  system, our calculated results represented by dashed blue and black curves for the

semiclassical and coupled-channel calculations without including coupling, respectively. The solid blue and black curves are the calculations including the coupling effects for the semiclassical and coupled-channel calculations, for the total fusion reaction cross section  $\sigma_{\text{fus}}$ , respectively, compared with the respective measured data (solid circles) in Fig. 1 panel (a). The experimental data for this system are obtained from Ref. [17]. The coupled-channel calculations using CCFULL performed by considering rotational deformations for both the projectile and target nuclei with deformations parameters  $\beta_2$ , and  $\beta_4$  adopted from Moller et al. [31] as listed in Table 2.

The position of the experimental Coulomb barrier  $V_b$  indicated by an arrow at the  $E_{\text{c.m.}}$  axis. In the case of no-coupling both semiclassical and quantum mechanical calculations underestimate the experiential data below the Coulomb barrier. The semiclassical calculations are markedly enhanced over the coupled-channel calculations below the Coulomb barrier when we had considered coupling effects. It is clearly seen that, the semiclassical calculations are in better agreement with the measured data compared to the coupled-channel calculations. Panel (b) of Fig. 1 shows the fusion barrier distribution  $D_{\text{fus}}$  calculations; we could not construct the second derivative accurately using the three-point difference method from the measured data due to few experimental data points for this system. In the corresponding results of the barrier distribution in the lower panel of Fig. 1 we are unable to make clear judgment, if our semiclassical calculations are more satisfactorily fitting the measured data than the coupled-channel calculations.

In a similar analysis, we compare our calculated results of  $\sigma_{\text{fus}}$  and  $D_{\text{fus}}$  with the corresponding data in panels (a) and (b) of Fig. 2, respectively, for the  ${}^8\text{He} + {}^{197}\text{Au}$  system. The experimental data of this system are obtained from Ref. [32]. In this case also, we had found that the inclusion of the coupling enhances the semiclassical calculations markedly above and below the Coulomb barrier compared with the measured data, while the CC calculations have very slight improvement below the Coulomb barrier, but still far from the measured data. This system also has few experimental data, that the construction of the second derivative is inaccurate; therefore, we cannot make clear judgment if our semiclassical or coupled-channel calculations are able to fit the measured data for the fusion barrier distribution calculations.

**Table 1** The parameters of Aküz-Winther potential along with  $V_b$  and  $R_b$

| Projectile + target                 | $V_0$ (MeV) | $a_0$ (fm) | $r_0$ (fm) | $V_b$ (MeV) | $R_b$ (fm) |
|-------------------------------------|-------------|------------|------------|-------------|------------|
| ${}^6\text{He} + {}^{238}\text{U}$  | 157.4       | 0.67       | 1.2        | 19.6        | 12.8       |
| ${}^8\text{He} + {}^{197}\text{Au}$ | 55.8        | 0.64       | 1.17       | 18.62       | 11.53      |

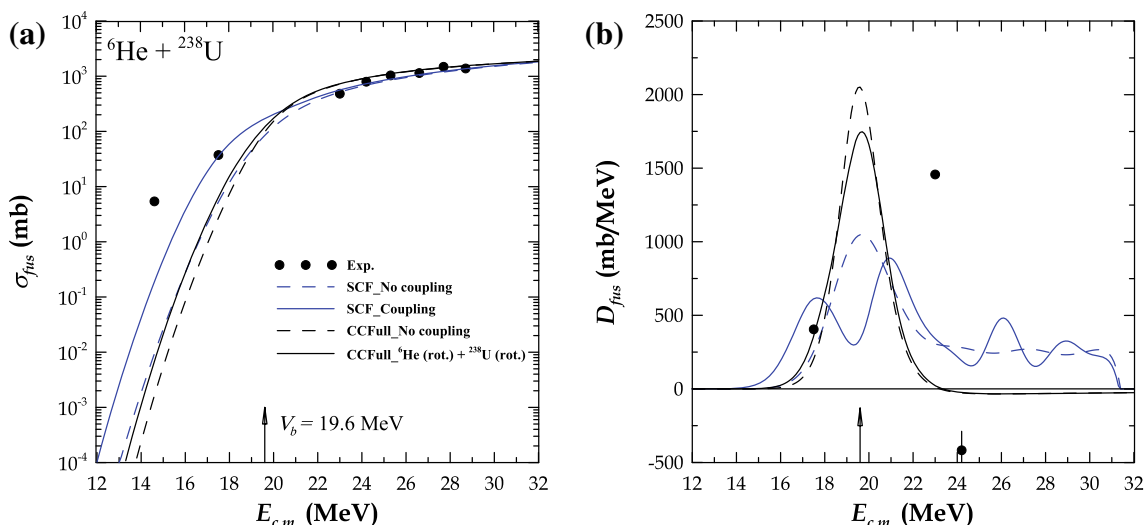


**Fig. 1** The comparison of the semiclassical and full quantum mechanical calculations using SCF code (blue curves) and CCFull code (black curves) with the experimental data (black filled circles) [17] for  ${}^6\text{He} + {}^{238}\text{U}$  system. **a** for the total fusion cross

section  $\sigma_{fus}$  (mb), and **b** for the fusion barrier distribution  $D_{fus}$ (mb/MeV), and the arrow represents the position of the Coulomb barrier  $V_b$

**Table 2** Deformation parameters and number of rotational levels used for CCFULL code for the studied systems

| System                              | Projectile nucleus |           |            | Target nucleus |           |            |
|-------------------------------------|--------------------|-----------|------------|----------------|-----------|------------|
|                                     | $\beta_2$          | $\beta_4$ | $N_{rot.}$ | $\beta_2$      | $\beta_4$ | $N_{rot.}$ |
| ${}^6\text{He} + {}^{238}\text{U}$  | 0.00               | 0.00      | 1          | 0.242          | 0.078     | 4          |
| ${}^8\text{He} + {}^{197}\text{Au}$ | 0.00               | 0.00      | 1          | -0.131         | -0.031    | 4          |

### Conclusions

The effect of coupled channel between the elastic channel and the continuum is found to be very essential in the semiclassical calculations which leads to improvement in the total fusion reaction cross section  $\sigma_{fus}$  and the fusion barrier distribution  $D_{fus}$  around and below the Coulomb barrier and brings the theoretical results closer to the

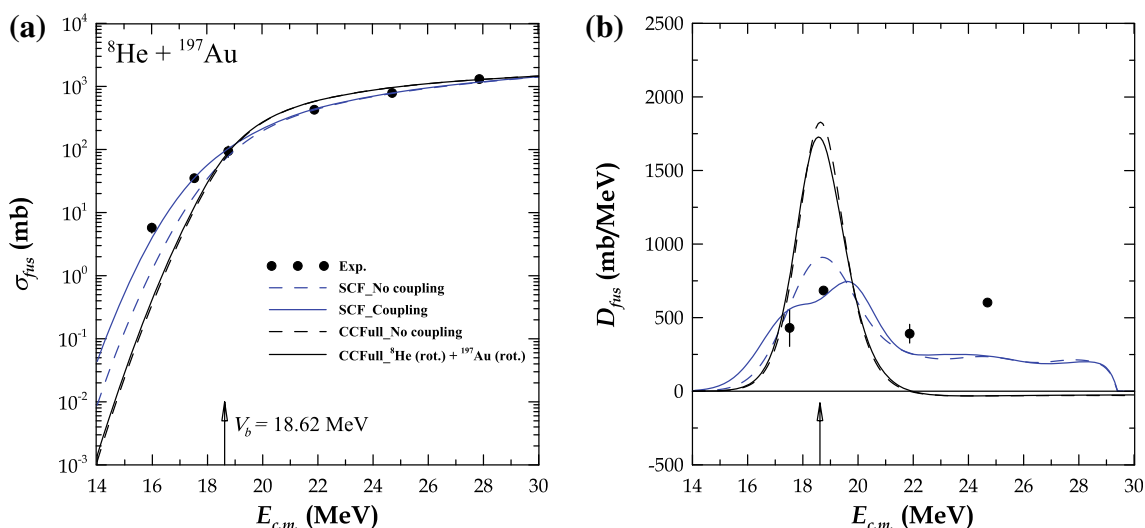


**Fig. 2** The comparison of the semiclassical and full quantum mechanical calculations using SCF code (blue curves) and CCFull code (black curves) with the experimental data (black filled circles) [32] for  ${}^8\text{He} + {}^{197}\text{Au}$  system. **a** for the total fusion cross

section  $\sigma_{fus}$  (mb), and **b** for the fusion barrier distribution  $D_{fus}$ (mb/MeV), and the arrow represents the position of the Coulomb barrier  $V_b$

experimental data. The inclusion of the coupling effects by considering both target and projectile have rotational deformations that enhances the full quantum mechanical calculations around and below the Coulomb barrier, but still have shortfall in reproducing data especially below the Coulomb barrier. The semiclassical approach used in the present work proves to be more adequate to describe light exotic nuclei than the full quantum mechanical ones in comparison with the experiment, because the semiclassical approach has been successfully extended to consider the continuum as a discrete set of channels as in Ref. [8]; therefore, the relative motion between the breakup fragments is more accurately described. The analytical continuation of the time variable is used to extend the trajectories to classically forbidden regions which enhances the calculations below the Coulomb barrier [25]. We could not construct the second derivative to calculate the fusion barrier distribution from the measured data accurately, therefore we could not make clear judgment of whether our semiclassical or coupled-channel calculations agreed with the experimental fusion barrier distribution. This work can be extended to study more systems involving halo nuclei, besides one can test its success or failure in the calculations of fusion reactions involving medium and heavy systems.

**Acknowledgments** The first author F.A.M. would like to acknowledge the financial support from Conselho Nacional de Desenvolvimento Científico e Tecnológico (CNPq) (Brazil) and is very grateful to the World Academy of Sciences for the advancement of science in developing countries (TWAS) (Italy) for a 1-year Grant under the scheme (TWAS-CNPq exchange programs for postdoctoral researchers).

**Open Access** This article is distributed under the terms of the Creative Commons Attribution 4.0 International License (<http://creativecommons.org/licenses/by/4.0/>), which permits unrestricted use, distribution, and reproduction in any medium, provided you give appropriate credit to the original author(s) and the source, provide a link to the Creative Commons license, and indicate if changes were made.

## References

- Canto, L.F., Gomes, P.R.S., Donangelo, R., Hussein, M.S.: Fusion and breakup of weakly bound nuclei. *Phys. Rep.* **424**, 1 (2006)
- Bertulani C. A., Hussein M. S., Münzenberg G.: *Physics of Radioactive Beams*. Nova Science, New York (2001)
- Bertulani, C.A., Canto, L.F., Hussein, M.S.: The structure and reactions of neutron-rich nuclei. *Phys. Rep.* **226**, 281 (1993)
- Hussein, M.S., Pato, M.P., Canto, L.F., Donangelo, R.: Near-barrier fusion of  $^{11}\text{Li}$  with heavy spherical and deformed targets. *Phys. Rev. C* **46**, 377 (1992)
- Hussein, M.S., Pato, M.P., Canto, L.F., Donangelo, R.: Real part of the polarization potential for  $^{11}\text{Li}$ -induced fusion reactions. *Phys. Rev. C* **47**, 2398 (1993)
- Takigawa, N., Kuratani, M., Sagawa, H.: Effect of breakup reactions on the fusion of a halo nucleus. *Phys. Rev. C* **47**, R2470 (1993)
- Dasso, C.H., Vitturi, A.: Does the presence of  $^{11}\text{Li}$  breakup channels reduce the cross section for fusion processes? *Phys. Rev. C* **50**, R12 (1994)
- Hagino, K., Vitturi, A., Dasso, C.H., Lenzi, S.M.: Role of breakup processes in fusion enhancement of drip-line nuclei at energies below the Coulomb barrier. *Phys. Rev. C* **61**, 037602 (2000)
- Diaz-Torres, A., Thompson, I.J.: Effect of continuum couplings in fusion of halo  $^{11}\text{Be}$  on  $^{208}\text{Pb}$  around the Coulomb barrier. *Phys. Rev. C* **65**, 024606 (2002)
- Diaz-Torres, A., Thompson, I.J., Beck, C.: How does breakup influence the total fusion of  $^{6,7}\text{Li}$  at the Coulomb barrier? *Phys. Rev. C* **68**, 044607 (2003)
- Mukherjee, A., Roy, S., Pradhana, M.K., Sarkar, M.S., Basua, P., Dasmahapatra, B., Bhattacharya, T., Bhattacharya, S., Basub, S.K., Chatterjee, A., Tripathi, V., Kailas, S.: Influence of projectile  $\alpha$ -breakup threshold on complete fusion. *Phys. Lett. B* **636**, 91 (2006)
- Dasgupta, M., et al.: Fusion and breakup in the reactions of  $^6\text{Li}$  and  $^7\text{Li}$  nuclei with  $^{209}\text{Bi}$ . *Phys. Rev. C* **66**, 041602(R) (2002)
- Dasgupta, M., et al.: Fusion versus breakup: observation of large fusion suppression for  $^9\text{Be}+^{208}\text{Pb}$ . *Phys. Rev. Lett.* **82**, 1395 (1999)
- Signorini, C., et al.: Does break-up affect  $^9\text{Be}$  fusion at the barrier?. *Eur. Phys. J. A* **5**, 7 (1999)
- Signorini, C.: Interaction at the barrier in the systems  $^{9,10,11}\text{Be}$ : well-established facts and open questions. *Eur. Phys. J. A* **13**, 129 (2002)
- Kolata, J.J., et al.: Sub-barrier fusion of  $^6\text{He}$  with  $^{209}\text{Bi}$ . *Phys. Rev. Lett.* **81**, 4580 (1998)
- Trotta, M., et al.: Large enhancement of the sub-barrier fusion probability for a halo nucleus. *Phys. Rev. Lett.* **84**, 2342 (2000)
- Alamanos, N., Pakou, A., Lapoux, V., Sida, J.L., Trotta, M.: Sub-barrier and near-barrier fusion study of halo nuclei. *Phys. Rev. C* **65**, 054606 (2002)
- Rehm, K.E., et al.: Fusion cross sections for the proton drip line nucleus  $^{17}\text{F}$  at energies below the Coulomb barrier. *Phys. Rev. Lett.* **81**, 3341 (1998)
- Kawai, M.: Chapter II. Formalism of the method of coupled discretized continuum channels. *Prog. Theo. Phys. Suppl.*, **89**, 1 (1986)
- Austern, N., et al.: Continuum-discretized coupled-channels calculations for three-body models of deuteron-nucleus reactions. *Phys. Rep.* **154**, 125 (1987)
- Nunes, F.M., Thompson, I.J.: Nuclear interference effects in 8B sub-Coulomb breakup. *Phys. Rev. C* **57**, R2818 (1998)
- Nunes, F.M., Thompson, I.J.: Nuclear interference effects in 8B sub-Coulomb breakup. *Phys. Rev. C* **59**, 2652 (1999)
- Alder, K., Winther, A.: *Electromagnetic Excitations*. North-Holland, Amsterdam (1975)
- Marta, H.D., Canto, L.F., Donangelo, R., Lotti, P.: Validity of the semiclassical approximation for the breakup of weakly bound nuclei. *Phys. Rev. C* **66**, 024605 (2002)
- Dasgupta, M., Hinde, D.J., Rowley, N., Stefanini, A.W.: Measuring barriers to fusion. *Annu. Rev. Nucl. Part. Sci.* **48**, 401 (1998)
- Morton, C.R., Berriman, A.C., Dasgupta, M., Hinde, D.J., Newton, J.O., Hagino, K., Thompson, I.J.: Coupled-channels analysis of the  $^{16}\text{O}+^{208}\text{Pb}$  fusion barrier distribution. *Phys. Rev. C* **60**, 044608 (1999)
- Leigh, J.R., Dasgupta, M., Hinde, D.J., Mein, J.C., Morton, C.R., Lemmon, R.C., Lestone, J.P., Newton, J.O., Timmers, H., Wei, J.X., Rowley, N.: Barrier distributions from the fusion of oxygen ions with  $^{144,148,154}\text{Sm}$  and  $^{186}\text{W}$ . *Phys. Rev. C* **52**, 3151 (1995)
- Canto, L.F., Donangelo, R., Marta, H.D.: Semiclassical treatment of fusion processes in collisions of weakly bound nuclei. *Phys. Rev. C* **73**, 034608 (2006) SCF code unpublished



30. Hagino, K., Rowley, N., Kruppa, A.T.: A program for coupled-channel calculations with all order couplings for heavy-ion fusion reactions. *Comput. Phys. Comm.* **123**, 143 (1999)
31. Moller, P., Nix, J.R., Myers, W.D., Swiatecki, W.J.: Nuclear ground-state masses and deformations. *At. Data Nucl. Data Tabl.* **59**(2), 185 (1995)
32. Lemasson, A., Shrivastava, A., Navin, A., et al.: Modern Rutherford experiment: tunneling of the most neutron-rich nucleus. *Phys. Rev. Lett.* **103**, 232701 (2000)

